Molecular Phylogenetics and Evolution 147 (2020) 106770

Contents lists available at ScienceDirect

Molecular Phylogenetics and Evolution

journal homepage: www.elsevier.com/locate/ympev

Genome-wide SNPs clarify lineage diversity confused by coloration in coralsnakes of the *Micrurus diastema* species complex (Serpentes: Elapidae)

Jacobo Reyes-Velasco[a,b,1], Richard H. Adams[a,1], Stephane Boissinot[b], Christopher L. Parkinson[c], Jonathan A. Campbell[a], Todd A. Castoe[a], Eric N. Smith[a,*]

[a] Department of Biology, University of Texas at Arlington, 501 S. Nedderman Drive, 337 Life Science, Arlington, TX 76010, USA
[b] New York University Abu Dhabi, Saadiyat Island, Abu Dhabi, United Arab Emirates
[c] Department of Biological Sciences and Department of Forestry and Environmental Conservation, Clemson University, 190 Collins St., Clemson, SC 29634, USA

ARTICLE INFO

Keywords:
Biogeography
Central America
Snake evolution
Systematics

ABSTRACT

New world coralsnakes of the genus *Micrurus* are a diverse radiation of highly venomous and brightly colored snakes that range from North Carolina to Argentina. Species in this group have played central roles in developing and testing hypotheses about the evolution of mimicry and aposematism. Despite their diversity and prominence as model systems, surprisingly little is known about species boundaries and phylogenetic relationships within *Micrurus*, which has substantially hindered meaningful analyses of their evolutionary history. Here we use mitochondrial genes together with thousands of nuclear genomic loci obtained via ddRADseq to study the phylogenetic relationships and population genomics of a subclade of the genus *Micrurus*: The *M. diastema* species complex. Our results indicate that prior species and species-group inferences based on morphology and color pattern have grossly misguided taxonomy, and that the *M. diastema* complex is not monophyletic. Based on our analyses of molecular data, we infer the phylogenetic relationships among species and populations, and provide a revised taxonomy for the group. Two non-sister species-complexes with similar color patterns are recognized, the *M. distans* and the *M. diastema* complexes, the first being basal to the monadal *Micrurus* and the second encompassing most North American monadal taxa. We examined all 13 species, and their respective subspecies, for a total of 24 recognized taxa in the *M. diastema* species complex. Our analyses suggest a reduction to 10 species, with no subspecific designations warranted, to be a more likely estimate of species diversity, namely, *M. apiatus*, *M. browni*, *M. diastema*, *M. distans*, *M. ephippifer*, *M. fulvius*, *M. michoacanensis*, *M. oliveri*, *M. tener*, and one undescribed species.

1. Introduction

The venomous coralsnakes of the family Elapidae comprise a diverse radiation of more than 170 taxa distributed in Southeast Asia and the New World (Campbell and Lamar, 2004; Castoe et al., 2007). Coralsnakes likely invaded the New World from Asia via a Beringian land bridge connecting Asia and North America during the late Oligocene (Kelly et al., 2009), similar to other major lineages of New World snakes (Castoe et al., 2007; Guo et al., 2012; Holman, 2000). Since their colonization of the New World, coralsnakes have diversified extensively across the Americas, into approximately 85 species in three genera (*Micruroides, Micrurus* and *Leptomicrurus*) that are now distributed from the US to Argentina (Campbell and Lamar, 2004). The genus *Micruroides* is composed of a single species (*M. euryxanthus*) and three subspecies that occur in western North America (Campbell and Lamar, 2004), while the genus *Leptomicrurus* consists of four South American species, although this group is sometimes synonymized with *Micrurus* (Slowinski, 1995; Uetz and Jirí, 2015). The vast majority of New World coralsnakes belong to the genus *Micrurus,* which is composed of approximately 80 recognized species (Uetz and Jirí, 2015).

Although the phylogenetic relationships among the major coralsnake lineages and other elapid snakes are relatively well understood (Castoe et al., 2007; Kelly et al., 2009; Keogh, 1998; Slowinski and Keogh, 2000a), little is currently known about the species-level relationships within the genus *Micrurus*. Despite the high diversity and broad distribution of *Micrurus*, external morphology is highly conserved across species (Campbell and Lamar, 2004). This lack of external morphological variation has led to a taxonomy that is largely defined by

* Corresponding author.
E-mail address: e.smith@uta.edu (E.N. Smith).
[1] These authors contributed equally.

https://doi.org/10.1016/j.ympev.2020.106770
Received 22 May 2019; Received in revised form 6 February 2020; Accepted 14 February 2020
Available online 18 February 2020
1055-7903/

color and color pattern variation (Roze, 1967, 1996). Indeed, the majority of systematic assessments of *Micrurus* have been based largely on phenotype (e.g. color, scalation, immunological assays, hemipene morphology, etc.), while only a small number of molecular studies exist, which are largely restricted in number of species and/or geographic sampling (Castoe et al., 2007; Castoe et al., 2012; Slowinski and Keogh, 2000b; Streicher et al., 2016).

Previous studies of the genus *Micrurus* proposed four main species groups that are defined largely based on broad color patterns: the monadal and bicolor groups, and the Central and South American triadal groups (Campbell and Lamar, 2004). Monadal coralsnakes are defined by a banding pattern consisting of a single black ring followed by a yellow and a red ring (i.e., the "classic" coralsnake pattern). The bicolor group includes a handful of species with a bicolor pattern of dark and pale rings, while members of the two triadal groups exhibit a pattern consisting of three black rings interspaced with pale colored rings followed by a red ring (Campbell and Lamar, 2004). These major groups are often subdivided into smaller subclades thought to represent groups of closely related species, as for example, the *M. diastema, M. tener* and *M. nigrocinctus* "species groups" that are often recognized within the monadal coralsnakes (Castoe et al., 2012; Lavin-Murcio and Dixon, 2004; Streicher et al., 2016).

The *Micrurus diastema* species group, herein defined, comprises 13 currently-recognized species and multiple subspecies that range from the southern U.S. to Honduras, with most taxa occurring in Mexico and northern Central America (Campbell and Lamar, 2004). These 13 species include *M. bernadi, M. bogerti, M. browni, M. diastema, M. distans, M. ephippifer, M. fulvius, M. hippocrepis, M. nebularis, M. pachecogili, M. proximans, M. stuarti* and *M. tener*. This group currently lacks any formal taxonomic classification, although many of its members were once considered conspecific or synonyms of *M. diastema* (Roze, 1967; Zweifel, 1959). Furthermore, there is considerable color variation both between and within species, which has complicated taxonomic resolution. For example, some species exhibit substantial variation in color pattern across their range and occasionally even within a single locality (Fraser, 1973). Conversely, other presumably more distantly-related and allopatric species often possess very similar color patterns (see example photographs in Campbell and Lamar, 2004).

Here we conduct a systematic evaluation of the *M. diastema* species group using thousands of genomic loci obtained via double digest restriction-site associated DNA sequencing (ddRAD-seq), together with sequences from two mitochondrial gene fragments. We use these data to infer phylogenetic relationships and species boundaries within the complex – effectively representing the first time that molecular data have been used to test long-standing taxonomic and systematic hypotheses otherwise based on coloration and morphology. Our analyses of molecular data for this group were designed to address the following questions: 1) Does the *M. diastema* species complex represent a natural monophyletic radiation? 2) Do current estimates of species limits defined largely by color patterns represent discrete genetically isolated lineages? 3) How many species should be recognized within this species complex?

2. Materials and methods

2.1. Taxon sampling and DNA extraction

We obtained tissues from a total of 116 samples from all species and subspecies of the *M. diastema* species complex (Fig. 1; Table S1), as well as from several outgroups. We collected these samples in Mexico and Central America between 1997 and 2015, and received additional tissue samples from multiple institutions. Tissue samples of blood, liver, skin or shed skin were preserved by snap freezing, kept dry (sheds or road kills), or preserved in lysis buffer, 100% EtOH or RNA*later* (Thermo Fisher Scientific). In some cases, skins were obtained and stored dry (e.g., shed skins). We isolated genomic DNA using the following methods: Qiagen DNeasy extraction kit (Qiagen, Inc., Valencia, CA, USA), Zymo Research Genomic DNA Tissue MiniPrep kit (Zymo Research Corporation, Irvine, CA, USA), standard phenol-choroform-isoamyl alcohol extraction (PCI), or with the use of AgenCourt Ampure XP DNA beads (Beckman Coulter, Inc., Irving, TX, USA).

2.2. Mitochondrial locus amplification and sequencing

We used polymerase chain reaction (PCR) to amplify a fragment of the mitochondrially-encoded NADH dehydrogenase subunit 4 (ND4) using the primers ND4 and Leu (Arèvalo et al., 1994), as well as Cytochrome Oxidase B (CytB) with the primers Gludg and ATRCB3 (Parkinson et al., 2002). We performed PCR reactions in total volumes of 25 μl using Takara Taq polymerase (Clonetech). Amplification included the following PCR conditions: initial denaturation step at 96 °C for 2 min, 35 cycles of denaturing at 95 °C for 15 s, annealing at 48 °C for one minute, and extension at 72 °C for two minutes, and a final extension at 72 °C for 10 min. Amplification products were purified using AgenCourt AMPure XP beads (Beckman-Coulter, Inc., Irving, TX, USA). Purified PCR products were then sequenced in both directions using the amplification primers and BigDye on an ABI 3730 capillary sequencer (Life Technologies, Grand Island, NY, USA). All sequences are deposited and available at NCBI's Genbank (Table S1).

2.3. ddRAD-seq library preparation and sequencing

We generated double digest restriction associated DNA (ddRAD) libraries for a subset of the samples (n = 56; Table S2) following the protocol of Peterson et al. (2012). We chose these 56 samples to include representative samples of all putative species and as many mitochondrial clades as possible (see below), while also working within the constraints of DNA quality and quantity per sample (some samples yielded low amounts of highly degraded DNA that was insufficient for ddRADseq). Genomic DNA was digested using a combination of a rare (*SbfI;* 8 bp recognition site) and common (*Sau3AI*; 4 bp recognition site) cutting restriction enzymes. We then ligated double-stranded indexed DNA adapters to the ends of digested fragments using a mixture of digested DNA, adapters, T4 Ligase enzyme, and T4 Ligase Buffer (New England Biolabs, Ipswich, MA, USA). These indexes also contained unique molecular identifiers (UMIs; eight consecutive N's upstream of the ligation site). We performed ligations on a thermal cycler at 16 °C for one hour, followed by a 10 min enzyme heat kill step at 65 °C. After adapter ligation, individual samples were pooled into groups of eight. We then size selected for a fragment size between 450 and 550 bp using a Pippin Prep (Sage Science, Beverly, MA, USA) and amplified the post-size selected pools using PCR with primers that included the remaining Illumina adapters and an index specific to each sub-pool. We then re-pooled the different sub-pools of samples in equimolar ratios based on molarity calculations from analysis on a Bioanalyzer DNA 7500 (Agilent, Santa Clara, CA, USA). The final pools were sequenced on two lanes of an Illumina HiSeq 2500 using 100 bp paired-end reads. Raw sequence reads are deposited in NCBI's Sequence Read Archive (SRA) under the accession number SRP129933 (Table S1).

2.4. mtDNA sequence analysis

We edited the raw mitochondrial ND4 and CytB sequence chromatograms using the program Geneious v6.1.6 (Biomatters Ltd., Auckland, NZ) and aligned the edited sequences using MUSCLE 3.5 (Edgar, 2004), followed by manual trimming of the 5′ and 3′ ends of each sequence to reduce columns with high levels of missing data. We concatenated both genes using the program SequenceMatrix (Vaidya et al., 2011). We included a single representative of the Guerrero Long-tailed rattlesnake, *Crotalus ericsmithi,* the Japanese coralsnake, *Sinomicrurus japonicus,* and the Sonoran coralsnake, *Micruroides euryxanthus* as outgroup taxa in the alignment. We also included 13 additional species of *Micrurus* obtained

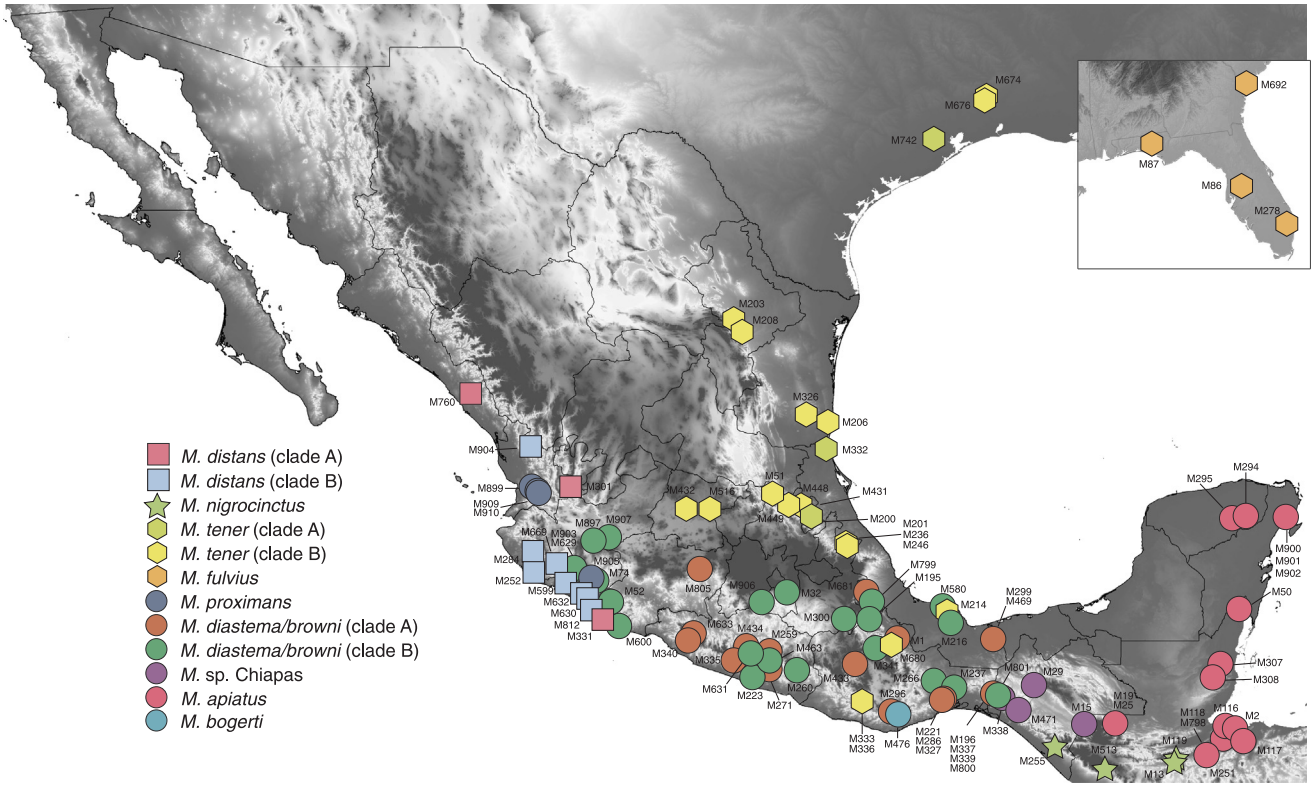

Fig. 1. Sample localities of *Micrurus* individuals sequenced in this study for mtDNA. Symbols represent group placement of each sample in the Bayesian phylogenetic inference analysis of mtDNA (Fig. 2).

from Genbank that are not considered part of the *M. diastema* species group. The final mtDNA dataset consisted of 669 bp for ND4 and 711 bp for CytB, for a total length of 1380 bp. Locality data for all samples, together with Genbank reference numbers, are provided in Table S1.

We used Bayesian Information Criterion (BIC) implemented in PartitionFinder v1.1.1 (Lanfear et al., 2012) to select best-fit models of evolution for each gene and codon position. The best-fit partition scheme for the alignment consisted of 6 partitions (one for each of the 3 codon positions for both genes), and the associated substitution models were HKY + Γ for 1st codon positions, HKY for the 2nd codon positions and GTR + Γ for 3rd codon positions for both mitochondrial genes. We used this best-fit partition scheme and set of substitution models to estimate phylogenetic relationships among members of the *M. diastema* complex using Bayesian Markov Chain Monte Carlo (MCMC) simulation in MrBayes v3.2.1 (Huelsenbeck and Ronquist, 2001), implemented on the CIPRES science gateway server (Miller et al., 2010). MrBayes analyses consisted of four independent runs, each of 10^7 MCMC generations with four chains (one cold and three heated), sampling every 1000th generation. We confirmed convergence of runs based on overlap in likelihoods and parameter estimates among runs, as well as effective sample size (ESS) and potential scale reduction factor value estimates (PSRF) values for each parameter, which were evaluated in Tracer v1.5 (Drummond and Rambaut, 2007). PSRF indicated that individual runs had converged by 10^5 generations (ESS $>$ 200 for all parameters), and we discarded the first 10^5 samples as burn-in. We combined the 4 independent MCMC samples (post burn-in) and computed a maximum clade credibility tree using TreeAnnotator v1.8.2 (Rambaut et al., 2014).

2.5. Processing and analysis of ddRAD-seq data

We processed the raw ddRADseq Illumina sequencing reads using the *ipyrad* 0.6.17 pipeline (Eaton and Overcast, 2017). We used this pipeline because it is designed and well-suited for inferring phylogenetic relationships between highly divergent taxa (Leaché et al., 2015). First, we trimmed restriction sites in all sequences using the FASTX toolkit (Gordon and Hannon, 2010). We then assembled loci *de novo* and extracted SNPs using *ipyrad* with the following quality-control options: we only kept sequences with an average *phred* score offset of 33, with fewer than 5 low quality base calls per read, and we used a clustering threshold of 85%. In order to understand the potential impacts of missing data on downstream analyses, we generated two different datasets based on the amount of missing data permitted (either 50% or 30% missing data allowed per locus, respectively). Because we found no substantial differences between inferences derived from the two datasets, we present results solely based on the 50% missing data dataset because it contained more loci (50% missing = 4975 loci versus 1807 loci in the 30% missing data dataset). Streicher et al. (2015) showed that a threshold of 50% missing data is adequate for phylogenomic studies.

In addition to our new data, we included additional ddRADseq data from 12 individuals of the *M. tener* species group from a recent study that used the same ddRADseq protocol (Streicher et al., 2016). After eliminating multiple individuals based on low coverage or low read quality, our final ddRADseq dataset included 60 individuals of coralsnakes (Tables S1 & S2): 48 newly sequenced samples and an additional 12 samples from Streicher et al. (2016). After quality filtering, we retained a total of ~110 million sequencing reads and a mean of ~20,000 RAD loci per individual. These data produced between 1198 and 4885 polymorphic loci and 12,847–38,497 SNPs per individual (Tables S2–S7). Our final dataset consisted of 4975 RADseq loci that were used for downstream inferences. Additionally, we generated a second alignment consisting of 4975 presumably unlinked biallelic SNPs, which we obtained by randomly sampling a single biallelic SNP from each variable RAD locus.

2.6. Phylogenetic analysis of SNP data

To provide a broad perspective on the overall phylogenetic diversity of this clade based on the SNPs resulting from the nuclear RADseq data, we estimated a maximum likelihood (ML) tree using a single SNP per locus (4975 SNPs). We used BIC model selection implemented in PAUP* v.4.0.a151 (Swofford, 2003) to estimate the best-fit model of sequence evolution, which selected the GTR + Γ + I model. We estimated a ML phylogeny using RAxML v8 (Stamatakis, 2014) on the CIPRES Science gateway server (Miller et al., 2010) with 1000 bootstrap replicates to assess nodal support. In order to better understand the effects of missing data in the ML topology, we re-ran RAxML using the 30% missing data dataset (1807 loci). Additionally, we used the NeighborNet algorithm in SplitsTree 4 (Huson and Bryant, 2005; Huson and Bryant, 2006) to construct a phylogenetic network using our alignment of 4975 SNPs.

2.7. Population STRUCTURE and nucleotide diversity

We inferred population structure and population assignments using three different approaches. First, we used STRUCTURE (Pritchard et al., 2000) and our 4975 biallelic SNP dataset. We first estimated the allele frequency distribution parameter (λ) by running an initial pilot run of STRUCTURE to infer λ with a $k = 1$, which inferred λ = 0.4239. We used this value for all subsequent runs. Based on preliminary results we found that *M. browni importunus* is more closely related to *M. nigrocinctus,* so we removed this samples from all subsequent STRUCTURE analyses. We ran STRUCTURE across a range of k values (k = 1–17) under mixed ancestry and single population models with all 59 samples. For all runs, we used the admixture model with correlated allele frequencies, a burn-in period of 50,000 MCMC followed by additional 50,000 iterations, and conducted 10 replicated analyses for each value of k. We used the ΔK method (Evanno et al., 2005) to estimate the most likely number of genetic clusters, and we also report the highest number of genetic clusters that make biological sense (Meirmans, 2015). Preliminary analyses suggested that members of the *M. diastema* species group into four main clades (see results). In order to increase the number of loci shared among individuals and to dissect fine-scale evidence of substructure within clades, we analyzed population structure in a hierarchical fashion, running the ipyrad pipeline, as previously described, to generate four clade-specific datasets for sets of individuals that comprised the following four main clades: *M. browni* group (n = 20), *M. diastema* group (n = 20), *M. distans* group (n = 6), and *M. tener* group (n = 12) as identified in our initial STRUCTURE analyses (i.e., including all 59 individuals). Using these four new clade-specific SNP datasets, we reran STRUCTURE using multiple values of k for each clade independently. We repeated these same analyses but included only loci present in all individuals of each particular species group to evaluate any impacts of missing data. We then used the adegenet package in R (Jombart, 2008) to perform discriminant analysis of principal components (DAPC) (Jombart et al., 2010) on the population clusters identified in the STRUCTURE analyses. However, we excluded samples with only a single individual. We used the optim.a.score function to determine the optimal number of PCs to retain that best describe the population structure without overfitting. Additionally, we ran the package fineRADstructure (v. 0.2) (Malinsky et al., 2018) to further investigate structure in the *M. diastema* species complex. Individuals were assigned to populations using 100,000 iterations as burn-in, followed by sampling of 100,000 MCMC iterations, and final trees were constructed using these 100,000 iterations. We visualized the output using the fineradstructureplot.r and finestructurelibrary.r R scripts (http://cichlid.gurdon.cam.ac.uk/fineRADstructure.html) in Rstudio (Team RStudio, 2015). In order to supplement our model-based population structure analyses, we conducted principle component analysis (PCA) using the base functions in R for the 4975 SNPs (Novembre et al., 2008). Finally, we used the program VCFTOOLS (Danecek et al., 2011) to calculate Weir and Cockerman's mean and weighted FST values among each species in the *M. diastema* species complex.

2.8. Coalescent-based species delimitation from SNP data

We used our biallelic SNP dataset to conduct Bayesian coalescent-based species delimitation using the BFD* method (Leaché et al., 2014) for two independent analyses: the *M. diastema* group (1–3 species; 2890 SNPs) and the *M. browni* group (1–2 species; 2033 SNPs).

The multispecies coalescent model implemented in BFD* assumes that species are reproductively isolated from one another (Yang and Rannala, 2010; Zhang et al., 2011). Based on this assumption, we designed species models to exclude individuals with evidence of mixed ancestry by excluding any individuals from BFD* analyses whose major population assignment probability was less than 95%. Due to this filtering scheme, we were unable to test the species validity of *M. apiatus*, *M. bernadi*, *M. nebularis*, and *M. bogerti* using BFD* because these putative taxa did not have more than one individual that passed this filtering criteria based on our sampling. We used the results of our STRUCTURE analyses to design and test 5 different competing species models for the *M. diastema* group, which represented alternative splitting/lumping individuals of *M. aglaeope* (n = 6), *M. diastema* (n = 3), and *M.* sp. Chiapas (n = 3) into respective species. Similarly, our *M. browni* analyses compared support for two competing models that consisted of either lumping or splitting *M. ephippifer* (n = 3) and *M. cf. proximans* (n = 7). Because BFD* also requires an outgroup, we used three individuals sampled from *M. proximans* as an outgroup taxon for our *M. diastema* analyses, and three individuals sampled from *M. diastema* as an outgroup for our *M. browni* analyses. Our species delimitation analyses focused on individuals within two species clusters of the *M. diastema* species group (*M. diastema* and *M. browni*), and we did not conduct BFD* analyses of *M. distans, M. fulvius,* or *M. tener* because our preliminary results indicated that these taxa are distantly related to the rest of the complex. Alternative species hypotheses that were tested are shown in Fig. S5.

For the BFD* analyses, we set $\alpha = 2$ and $\beta = 50$ for the gamma prior on the speciation rate parameter and $\alpha = 1$ and $\beta = 200$ for the effective population size parameter for each species. We conducted path sampling using the BFD* method as implemented in BEAST v2.4.8 (Bouckaert et al., 2014) to estimate marginal likelihoods for each species model, using a total of 48 steps, with each step consisting of 2.5×10^5 MCMC generations, and $\beta = 0.02$. We obtained marginal likelihood estimates after discarding the first 25% of MCMC samples as burn in for each step, which were then used to compute Bayes Factors between competing species models to identify the best-fit model for the two BFD* sets of analyses (*M. diastema* and *M. browni*). Bayes Factors were computed in relation to the model with the highest marginal likelihood estimate for the two analyses, respectively.

2.9. SNP-based species tree estimates and TreeMix analyses

We estimated a species-level phylogeny for the *M. diastema* species group using the program SVDquartets (Chifman and Kubatko, 2014) in PAUP* v.4.0.a151 (Swofford, 2003) and our 4975 biallelic SNP dataset, with species definitions based on the best-fit models inferred using our BFD* analyses described above and the results from the STRUCTURE analyses. We included individuals from the outgroup lineages *M. fulvius* (n = 5), *M. tener* (n = 8), and *M. distans* (n = 6), and used all possible quartets and 100 bootstrap replicates to assess topological support. Additionally, we inferred patterns of migration involving the nine putative species/populations with at least 2 individuals with the program TreeMix (Pickrell and Pritchard, 2012). We conducted TreeMix analyses using 11 different migration parameter settings, ranging from zero to 10 migration events. For each migration setting, we conducted 100 replicate analyses, and identified the highest likelihood run from this set of 100 to characterize evidence for the best-fit migration model.

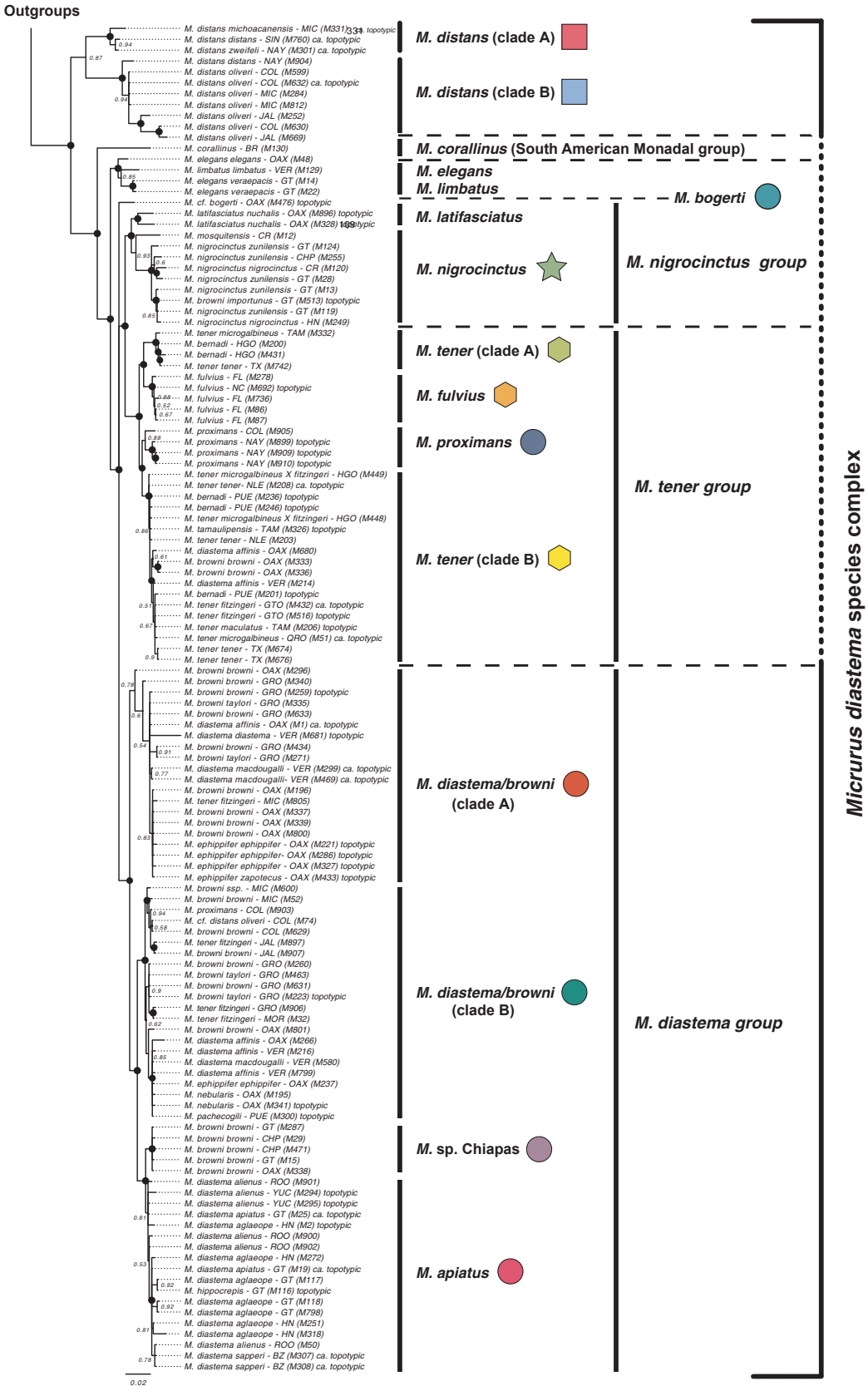

Fig. 2. Bayesian phylogenetic inference of the mitochondrial genes Cytb and ND4. Black circles represent nodes with posterior support > 0.95. Multiple currently recognized species are represented within each mtDNA clade. Species names at nodes are based on mophological identification of each individual. Species and group names indicated in this figure represent the initial taxonomy used.

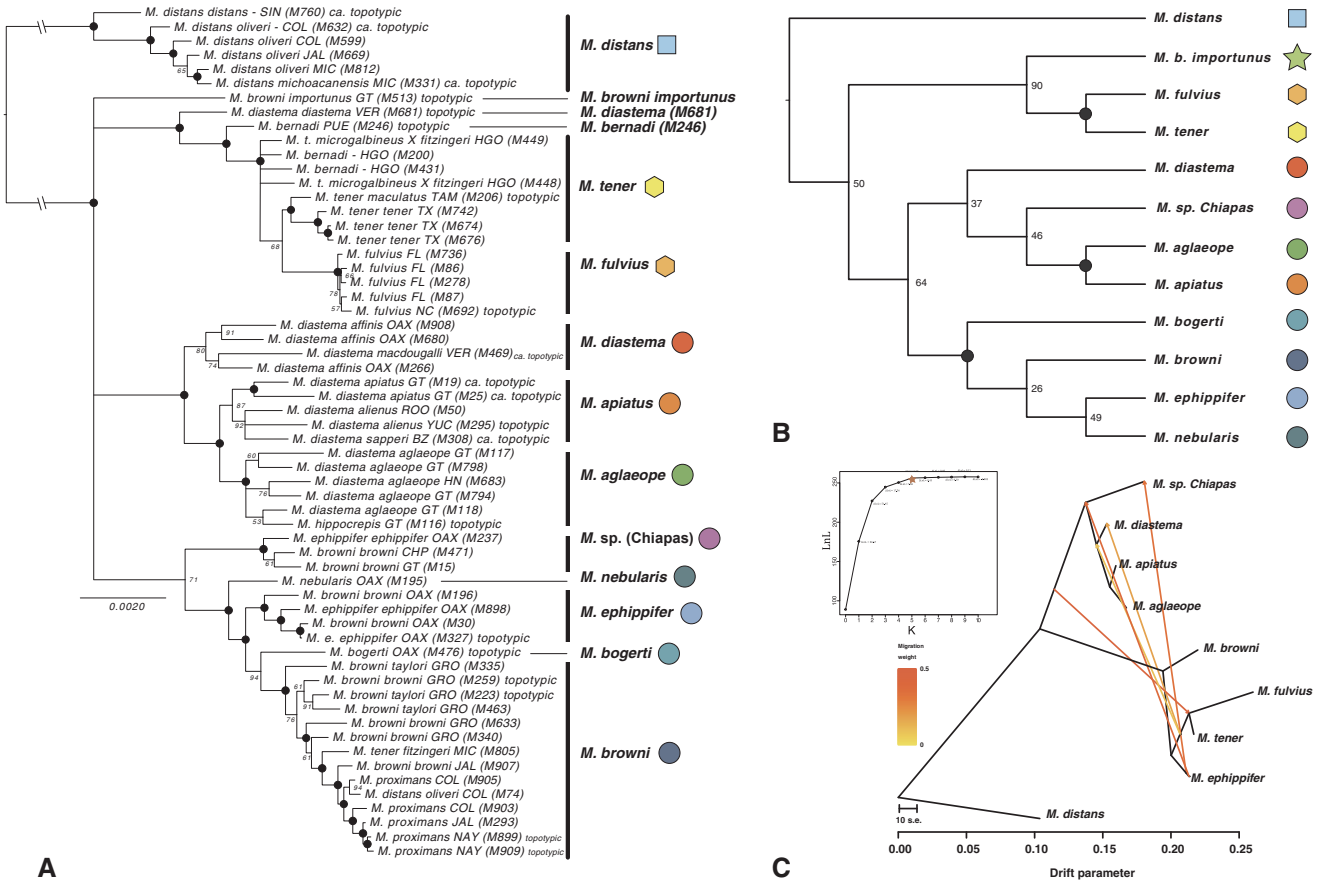

Fig. 3. (A) Maximum likelihood phylogenetic inference of the *M. diastema* species complex based on 4975 unlinked SNPs. Black circles represent nodes with > 95 bootstrap support (BS). We collapsed all nodes with bootstrap support values below 50. (B) SVDquartets species tree estimated for members of the *M. diastema* species complex. Numbers at nodes represent bootstrap support measured from 100 replicates. Black circles represent nodes with 100% bootstrap support. (C) TreeMix population-tree inferred using all loci that had at least one individual from each lineage. The phylogeny alone (without migration events) explains ~95.69% of the variance in SNP data, while the model including 5 migration edges explains ~99.96%. Migration events in the population tree are depicted by arrows. Inset graph depicts the changes in likelihood as a function of the number of migration events included in the model.

3. Results

3.1. mtDNA phylogenetic relationships

Our inferred mtDNA phylogeny provides evidence that many previously defined species and subspecies exhibit non-monophyletic mitochondrial haplotype groupings, particularly within the central and North American monadal coralsnakes (Fig. 2). We recovered strong support (PP > 0.95) for an early split between *M. distans* and all other species in the *M. diastema* species complex, as well as a deep divergence and polyphyletic relationships between central and South American monadal coralsnakes, represented in our analyses by *M. corallinus*; the central American monadal species (i.e., *M. nigrocinctus*, *M. tener*, and *M. diastema* groups) were instead inferred to be sister to a clade composed of *M. elegans* (triadal) + *M. limbatus* (bicolor), with strong support (PP > 0.95).

We inferred a strongly supported clade (PP > 0.95) of North American monadal species that includes *M. bernadi, M. fulvius,* and *M. tener*—we refer to this clade as the *M. tener* group (Fig. 2). An individual of *M. diastema* from Veracruz (M680) and two individuals of *M. browni* cf. *bogerti* from Oaxaca (M333 and M336) were nested within the *M. tener* group, with strong support (PP > 0.95). We found evidence that *M. tener* itself is largely comprised of two distinct and polyphyletic mitochondrial haplogroups ("*M. tener* clade A" and "*M. tener* clade B"), as previously reported by Streicher et al. (2016), and we also found that mitochondrial haplotypes of *M. proximans* were inferred as the sister lineage to one these *M. tener* haplogroups ("*M. tener* clade B"; Fig. 2). The *M. tener* group was inferred to be the sister clade to the Central American *M. nigrocinctus* group, while an individual haplotype of the subspecies *M. browni importunus* (M513) was nested within *M. nigrocinctus,* with strong support (PP = 1).

All the remaining members of the *M. diastema* species complex formed a distinct and strongly supported clade, which we refer to as the "*M. diastema* group", which includes individuals from *M. browni, M. diastema, M. ephippifer, M. hippocrepis, M. nebularis,* and *M. pachecogili,* as well as an individual identified as *M. proximans* from Colima, Mexico (M903) and one individual previously referred to as *M. tener* from Morelos, Mexico (M32; Fig. 2). All subclades within this *M.* diastema group were comprised of individuals that generally corresponded well with geographic proximity but not with historically recognized species or subspecies designations. For example, we found that many individuals identified as *M. diastema* were clustered with samples identified as *M. browni*, *M. hippocrepis* or *M. ephippifer* (Fig. 2). Within this larger *M. diastema* group, our mtDNA phylogenetic analyses infer four major subclades, the majority of which were strongly supported (PP > 0.95; Fig. 2).

We inferred a clade that comprised *M. browni* individuals from Michoacán, Guerrero and Oaxaca, *M. ephippifer* from Oaxaca, and *M. diastema* from Veracruz and Oaxaca—we refer to this group as "*M. diastema/browni* clade A". However, this clade received low support (PP < 0.95). We recovered a second mtDNA cluster that included individuals of *M. browni* from Jalisco to Oaxaca, *M. nebularis, M. pachecogili,* as well as several individuals of *M. diastema* from Oaxaca and Veracruz, an individual of *M. ephippifer* from Oaxaca (M237), one *M.*

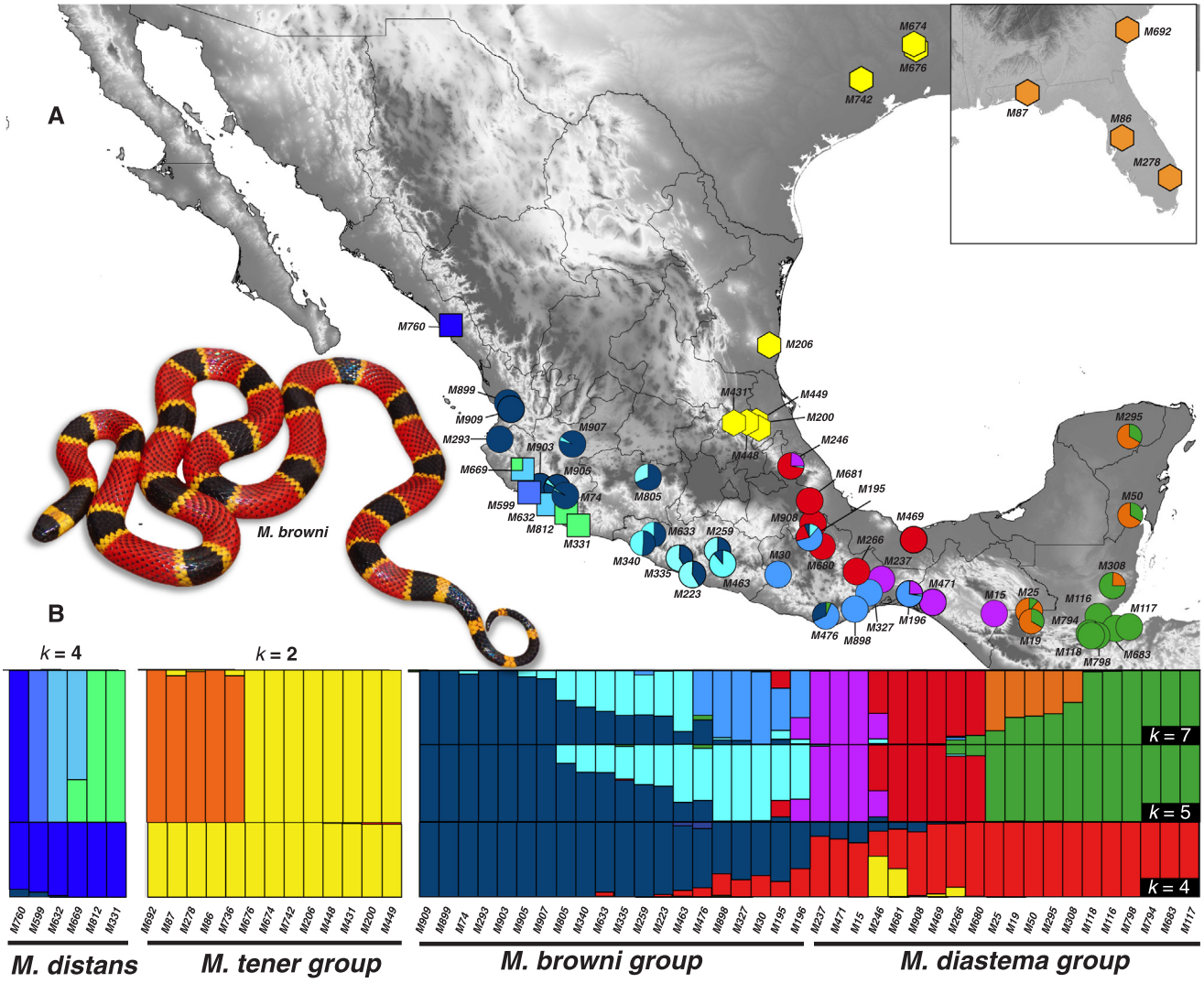

Fig. 4. (A) Locality map of individuals of *Micrurus* included in the ddRADseq analyses. Colors correspond to the proportion of ancestry as inferred in the STRUCTURE analyses with $k = 7$ for the *M. browni* and *M. diastema* groups, $k = 4$ for the *M. distans* group, and $k = 2$ for the *M. tener* group. (B) Bar plot showing the inferred ancestry of 59 individual genotypic profiles of members of the *M. diastema* species complex resulting from different analyses in the program STRUCTURE. The first (bottom) was inferred from 4975 unlinked SNPs across all 59 individuals. The most supported value was $k = 4$. The second analysis (middle) included only those individuals of each one of the four major species groups: *M. diastema* + *M. browni* groups (4849 SNPs; $k = 5$), *M. distans* (2317 SNPs; $k = 4$) and *M. tener* clade (7786 SNPs; $k = 2$). The third analysis (top) included those individuals of the *M. diastema* + *M. browni* groups (4849 SNPs; $k = 7$). Colors indicate the proportion of ancestry (q) attributed to each cluster.

proximans from Colima (M903) and an individual of *M. tener* from Morelos (M32). We refer to this clade as the "*M. diastema/browni* clade B". The two mtDNA clades of *M. diastema/browni* (clades A and B) were not sister to one another, as the *M. diastema/browni* clade B was sister to the two remaining clades with high posterior support (PP = 1). Of the remaining two clades within the *M. diastema* group, one clade included all *M. diastema* samples east of the Isthmus of Tehuantepec, including the Yucatan peninsula, and the subspecies *M. d. apiatus, M. d. aglaeope, M. d. alienus*, *M. d. sapperi,* as well as *M. hippocrepis*—we refer to this group as the "*M. apiatus*" clade. Lastly, we inferred a "*M. sp.* Chiapas" clade that includes individuals of *M. browni* from Chiapas, eastern Oaxaca and western Guatemala (excluding *M. browni importunus*). These last two clades were sister to one another, with strong support (PP = 1; Fig. 2).

3.2. Phylogenetic estimates from genome-wide SNP data

Our ML-analysis of the concatenated nuclear RAD loci recovered evidence of multiple, distinct clades, with many nodes exhibiting high bootstrap support (BS > 95; Fig. 3A). However, major relationships among the four major clades were poorly resolved, except for a well-supported division between *M. distans* and the other Central American monadal coralsnakes (Fig. 3A). We recover an almost identical topology when using the 50% or the 30% missing data datasets (see Fig. S1), so here we report the results of only the first dataset.

All members of *M. tener* and *M. fulvius*, plus individuals of *M. diastema* (M681) and *M. bernadi* (M246) clustered into a single clade with high support (BS > 95). Within the *M. diastema* group, we found a number of conflicting relationships between our mitochondrial and nuclear phylogenies (i.e., Fig. 2 vs. Fig. 3). For example, the "*M. sp.* Chiapas" clade of our mitochondrial phylogeny was inferred to be sister to a clade largely comprised of *M. ephippifer* and *M. browni* samples in our concatenated nuclear loci tree (vs. sister to *M. apiatus* in the mitochondrial analyses), and *M. proximans* samples were found to be nested within a clade of *M. browni*, rather than within the *M. tener* group as inferred in the mitochondrial tree. Our concatenated nuclear tree shows two main clades: one Caribbean, including largely *M. diastema* populations previously recognized as subspecies, and one Pacific

main-clade, encompassing populations from the dry upper Grijalva Valley of Chiapas, the arid highlands of southern Mexico, and the xeric coast from western Chiapas to Nayarit. Within the Caribbean main-clade, also corresponding to discrete phylogenetic clusters that follow geographic subdivisions: a western clade including individuals from Gulf of Mexico populations from Oaxaca and Veracruz (*M. diastema*), and an eastern clade, including individuals from the Yucatan Peninsula to northwestern Honduras. Within this eastern clade of *M. diastema*, we found that samples from regions in and around the Yucatan peninsula formed a clade ("*M. apiatus*"; BS = 87) that was sister to individuals from Caribbean Guatemala and Honduras ("*M. aglaeope*"; BS > 95; Fig. 3A). We also found that the single individual of *M. browni importunus* (M513) was not closely related to any other species in the *M. diastema* species complex, a similar result to our mtDNA phylogeny.

Our nuclear loci tree also resolved the Pacific main-clade, including *M. browni, M. proximans, M. ephippifer* and *M. nebularis*, as well as individuals previously identified as *M. tener* from Colima, and an individual identified as *M. bogerti*. This clade received low bootstrap support (BS = 71), when including *M. sp.* Chiapas. Within this group, we observed four distinct lineages showing geographic and taxonomic correspondence: the *M. sp.* (Chiapas) clade (upper Grijalva Valley and adjacent Isthmus of Tehuantepec), *M. nebularis* (Central Oaxacan highlands), the *M. ephippifer* clade (area comprising the Isthmus of Tehuantepec and adjacent highlands), and the *M. browni* clade (Pacific versant from western Oaxaca to Nayarit). The *M. sp.* (Chiapas) clade (BS > 95) comprised two individuals of *M. browni* from Chiapas and one *M. diastema* from Oaxaca (similar to our mtDNA analysis). The sole individual of *M. nebularis* (M195) formed the sister lineage to the *M. ephippifer* plus *M. browni* clades (Fig. 3A). Our SplitsTree network analysis of the same SNP dataset recovered effectively the same six major genetic groupings for individuals within the *M. diastema* species complex (Fig. S2), these results were also broadly consistent with inferences from STRUCTURE and coalescent-based analyses of the nuclear SNP data (shown below). It is notable, however, that results from STRUCTURE analyses (see below), which indicate mixed ancestry of a number of individuals, suggest that these nuclear trees/networks should be interpreted with caution.

3.3. Population structure and nucleotide diversity

The STRUCTURE analysis including all 59 samples best supported a value of $k = 4$ genetic clusters, based on the Evanno method (Fig. 4), which correspond to the *M. distans, M. tener, M. diastema* and *M. browni* species groups. This analysis shows admixture between the *M. tener* and the *M. diastema* group at the level of the Trans-Mexican Volcanic Belt (TMVB). A specimen of *M. bernadi* (M246) located north of the TMVB, a junior synonym of *M. tener sensu* Streicher et al. (2016), exhibited about a 30% *M. diastema* and 50% *M. tener* mixed ancestry. The near topotypic specimen of *M. diastema* (M681), from El Fortin, Veracruz, and just south of the TMVB, shows an opposite trending mixed ancestry, about 50% *M. diastema* and 30% *M. tener*. Because our mtDNA and nuclear SNP data suggested that each of these four groups contains multiple lineages, and to better dissect patterns of their intra-clade structures, we re-ran STRUCTURE analyses for the four major genetic clades independently. Clade-specific STRUCTURE analysis of the *M. distans* group favored a value of $k = 4$, with individuals from Sinaloa, Michoacán and Colima forming separate genetic clusters. However, most genetic clusters corresponded to single individuals and one individual from Colima showed mixed ancestry with samples from Michoacán. In the *M. tener* group, the STRUCTURE analysis favored a value of $k = 2$, which separated *M. fulvius* and *M. tener,* with only minor evidence of recent admixture between the two groups.

STRUCTURE analyses ran separately for the *M. diastema* and *M. browni* groups yielded identical results to those on the two groups separately, we thus only report results for the combined analysis here. The STRUCTURE analysis for the combined *M. diastema* and *M. browni* groups best supported a value of $k = 5$, with minor support for $k = 7$. Each genetic cluster largely corresponds to samples from particular geographic regions (Fig. 4A).

In the *M. browni* group for $k = 5$, we recovered evidence of two main genetic clusters with individuals of *M. ephippifer, M. diastema, M. nebularis* and some southern *M. browni* forming a group, and *M. proximans* and *M. browni* from Nayarit to Colima forming a separate cluster, while all individuals from Michoacán and Guerrero showed admixture between these two groups. At $k = 7$ however, individuals from Oaxaca (*M. ephippifer, M. diastema, M. nebularis* & *M. browni*) formed their own cluster, with high levels of admixture between three of the individuals (M195, M196 & M476) and other members of the *M. diastema* and *M. browni* groups, while members of *M. proximans* and *M. browni* showed a north to south gradient in assignment probability, with all samples from Michoacán and Guerrero showing evidence of admixture.

All the samples of *M. diastema* west of the Isthmus of Tehuantepec (west of the Tonalá River) grouped together into a single genetic cluster, while individuals from the central depression of Chiapas and the eastern Isthmus of Tehuantepec formed a distinct clade (*M.* sp. Chiapas). One individual of *M. bernadi* from Puebla (M246) showed evidence of mixed ancestry between the eastern *M. diastema* clade and the *M.* sp. Chiapas clade, although this could reflect the mixed ancestry between *M. tener* and *M. diastema* discussed above. All samples from the Yucatan peninsula, Guatemala and Honduras clustered together at $k = 5$. However, at $k = 7$, samples from Yucatan and western Guatemala (*M. apiatus*) separated from those in eastern Guatemala and Honduras (*M. aglaeope*), but with evidence of mixed ancestry between the two clades. STRUCTURE runs with no missing data (but very few loci) resulted in nearly identical results (Fig. S4), with a k of 4 as the most supported value of k in the *M. diastema* group and a $k = 2$ for the *M. browni* group, respectively. The resulting population assignments in DAPC recovered 4 populations as the most supported value of k, followed by a k of 5 and 6 (Fig. S3). These population assignments are mostly consistent with both the STRUCTURE analyses and fineRADstructure, which identified the same *M. browni, M. diastema, M. distans* and *M. tener* species groups. At a k of 5, DAPC recovered individuals of *M. tener* and *M. fulvius* as separate genetic clusters, while at a k of 6, DAPC split individuals of *M. browni* (and *M. proximans*) from *M. ephippifer*.

The fineRADstructure analysis was largely in agreement with the STRUCTURE and DAPC results (Fig. S6), as it identified four main groups, each one further subdivided into what generally corresponds to different species. We also detected varying levels of population genetic differentiation among members of the *M. diastema* species complex (Table 1). We observed the highest mean *Fst* values between *M. distans* and *M. fulvius,* and the lowest *Fst* between different subspecies of *M. diastema* (i.e., *M. d. aglaeope* and *M. d. apiatus,* mean *Fst* = 0.02).

3.4. Coalescent-based species delimitation

Both the *M. diastema* and *M. browni* group-specific analyses selected the largest number of species as their respective best-fit models (Fig. S5). For the *M. diastema* group-specific analyses, Bayes Factor comparison of species delimitation models identified 3 distinct species (*M. diastema*, *M. aglaeope*, and *M. sp.* Chiapas) that were inferred with strong support when compared to the second-best model consisting of 2 species (BF = −3522 for lumping *M. aglaeope* and *M. sp.* Chiapas). Similarly, a two-species model (*M. ephippifer* and *M. proximans*) was the best-fit model for our *M. browni* group-specific analyses (BF = −4237.4 for lumping *M. ephippifer* and *M. proximans*).

3.5. SNP-based species tree inference and migration edges

SVDquartets recovered a species-level phylogeny for the *M. diastema* group that was generally similar to our SplitsTree phylogeny and ML tree of concatenated ddRAD loci, with several minor differences:

Table 1
Fst values for species and populations of the M. diastema species complex as obtained from the ddRADseq SNP dataset. Numbers above the diagonal represent Weir and Cockerham's weighted Fst values, while numbers below the diagonal represent Weir and Cockerham's mean Fst values.

	M. d. aglaeope	*M. d. apiatus*	*M. browni*	*M.* sp. Chiapas	*M. d. diastema*	*M. distans*	*M. ephippifer*	*M. fulvius*	*M. tener*
M. d. aglaeope	–	0.08	0.54	0.36	0.19	0.72	0.40	0.67	0.53
M. d. apiatus	0.02	–	0.51	0.30	0.14	0.69	0.35	0.63	0.50
M. browni	0.27	0.26	–	0.56	0.47	0.82	0.34	0.74	0.61
M. sp. Chiapas	0.17	0.11	0.24	–	0.30	0.77	0.41	0.79	0.60
M. d. diastema	0.08	0.05	0.24	0.11	–	0.68	0.29	0.56	0.41
M. distans	0.46	0.41	0.53	0.56	0.41	–	0.78	0.88	0.80
M. ephippifer	0.20	0.16	0.14	0.22	0.13	0.55	–	0.74	0.55
M. fulvius	0.40	0.34	0.36	0.56	0.30	0.71	0.47	–	0.38
M. tener	0.27	0.25	0.27	0.31	0.20	0.50	0.27	0.12	–

individuals from Chiapas (*M. sp.* Chiapas) were recovered as the sister group to *M. diastema*, *M. apiatus* and *M. aglaeope,* with strong support (BS = 99), while this clade was sister to *M. nebularis, M. ephippifer, M. bogerti* and *M. browni* (Fig. 3B) in the concatenated ML-analysis. Additionally, *M. browni importunus* (represented by a single individual, M513) was recovered as sister to all other species, with the exclusion of *M. distans, M. fulvius* and *M. tener*, but with low support (BS = 51); in contrast, the concatenated nuclear ddRAD dataset inferred *M. browni importunus* as sister to *M. fulvius* and *M. tener,* but with very low support (BS < 50). Comparing the likelihood support of the 11 different TreeMix runs suggested a population tree model that includes 5 separate migration events (Fig. 3C), thus indicating evidence of potentially widespread gene flow among many populations. However, the population tree estimated recovered in TreeMix differed from our SVDquartets and the SNP ML phylogeny in that it recovered *M. fulvius* + *M. tener* as nested in the *M. browni* species group.

4. Discussion

4.1. Phylogenetic relationships of the Micrurus diastema species complex

Coralsnakes of the genus *Micrurus* represent a diverse group of highly venomous snakes that are involved in complex mimicry systems (Brodie III and Janzen, 1995; Pfennig et al., 2001a; Rabosky et al., 2016; Smith, 1975, 1977). Despite their medical importance, little was previously known about the phylogenetic relationships between North American members of the genus (Castoe et al., 2012; Streicher et al., 2016), because the few molecular studies to date have largely focused on higher-level relationships among coralsnakes and other Elapids (Castoe et al., 2007; Slowinski and Keogh, 2000a) or on other areas of the world (Jowers et al., 2019; Renjifo et al., 2012; Valencia et al., 2016). Due to the highly-conserved morphology of coralsnakes, much of the systematics of this large clade has historically relied heavily on color characteristics. However, multiple studies have shown that color patterns can be particularly plastic and under strong selection in snakes, and therefore may mislead taxonomy and inferences of relatedness (Brodie III, 1993; Cox and Davis Rabosky, 2013; Greene and McDiarmid, 1981a; Pfennig et al., 2001b; Rabosky et al., 2016). Our study shows that in the case of the *M. diastema* species complex, coloration has in fact misguided previous efforts to estimate the diversity of coral snakes and understand their evolutionary relationships.

Our phylogenetic inferences based on RADseq and mitochondrial loci provide new insight into the evolutionary history of the *M. diastema* species complex. First, both mtDNA and nuclear RADseq inferences suggest that, despite similar coloration patterns, *M. distans* is not closely related to any other members of the *M. diastema* species complex, as was previously assumed. Instead, our results indicate that *M. distans* is a deeply-divergent lineage that is the sister group to the majority of remaining monadal coralsnakes from North, Central and South America, as well as to *M. elegans* and *M. limbatus* from Middle America. We also find that multiple Central American species with a monadal color pattern, which we refer to as the *M. diastema* species complex (*sensu stricto*) are the sister group to the *M. tener* + *M. nigrocinctus* species groups. The *M. diastema* species complex is then composed of two main lineages. The first includes individuals previously assigned to *M. diastema* and *M. hippocrepis* from eastern Mexico, the Yucatan peninsula and Nuclear Central America, as well as what appears to be an undescribed species ("*M. sp.* Chiapas"). Within this lineage, we find evidence for strong genetic differentiation between populations east and west of the Isthmus of Tehuantepec (Fig. 3, Fig. 4, Fig. 5). We refer to this group as the *M. diastema* species group. The second lineage within the *M. diastema* species complex is composed of individuals that are mostly found in the west coast of Mexico, as well as in the central highlands, between the TMVB and the Isthmus of Tehuantepec (Fig. 3, Fig. 4). This lineage, which we refer to as the *M. browni* species group, contains multiple currently recognized species, including *M. browni, M. bogerti, M. nebularis, M. ephippifer, M. pachecogili* and *M. proximans*, however, we questioned the validity of several of these species.

4.2. Discrepancies between mtDNA and nuclear SNP phylogenies

Several notable discrepancies exist between our phylogenetic estimates obtained from mtDNA and nuclear SNP datasets. One example is the placement of *M. proximans*, which based on mtDNA data was recovered as sister to some members of *M. tener* (Fig. 2), while all nuclear SNP analyses suggest that *M. proximans* samples are nested within *M. browni* (Fig. 3, Fig. 4, Fig. 5). Another example of strong mito-nuclear disagreement was between samples of *M. diastema* and *M. browni* in southern Mexico (within and adjacent to the state of Guerrero; Fig. 1). Additional examples of conflict between our analyses of mtDNA and nuclear estimates include a near-topotypic individual of *M. diastema*, from El Fortin, Veracruz (M681), which shows evidence of mixed ancestry between *M. tener* and *M. diastema* in the STRUCTURE, SplitsTree Networks and PCA analyses (Fig. 4, Fig. S2, Fig. 5, respectively). The ML-analyses of the SNP data places this individual as the sister lineage to members of the *M. tener* group, with strong support (BS = 100), while it is nested with the *M. browni/diastema* A group in the mtDNA analyses (Fig. 2).

Our mtDNA phylogeny also recovered two distinct mitochondrial clades shared between members of both the *M. diastema* and *M. browni* groups (Fig. 1, Fig. 2). These two mitochondrial lineages occur in near sympatry in several areas of southern Mexico, especially in the states of Guerrero and Oaxaca (Fig. 1). However, our analyses of genome-wide SNP data recovered a very different topology, with individuals showing the same mtDNA haplogroups nested with either the *M. diastema* or *M. browni* groups (Fig. 3, Fig. 4).

These apparent conflicts between inferences derived from mitochondrial and nuclear genomes could be the result of a variety of factors (Som, 2014), including simple estimation error (Rannala and Yang, 2008), ancient or recent gene flow (Good et al., 2008), natural selection (Adams et al., 2018; Castoe et al., 2009), or incomplete lineage sorting (Kubatko and Degnan, 2007; Mendes and Hahn, 2016;

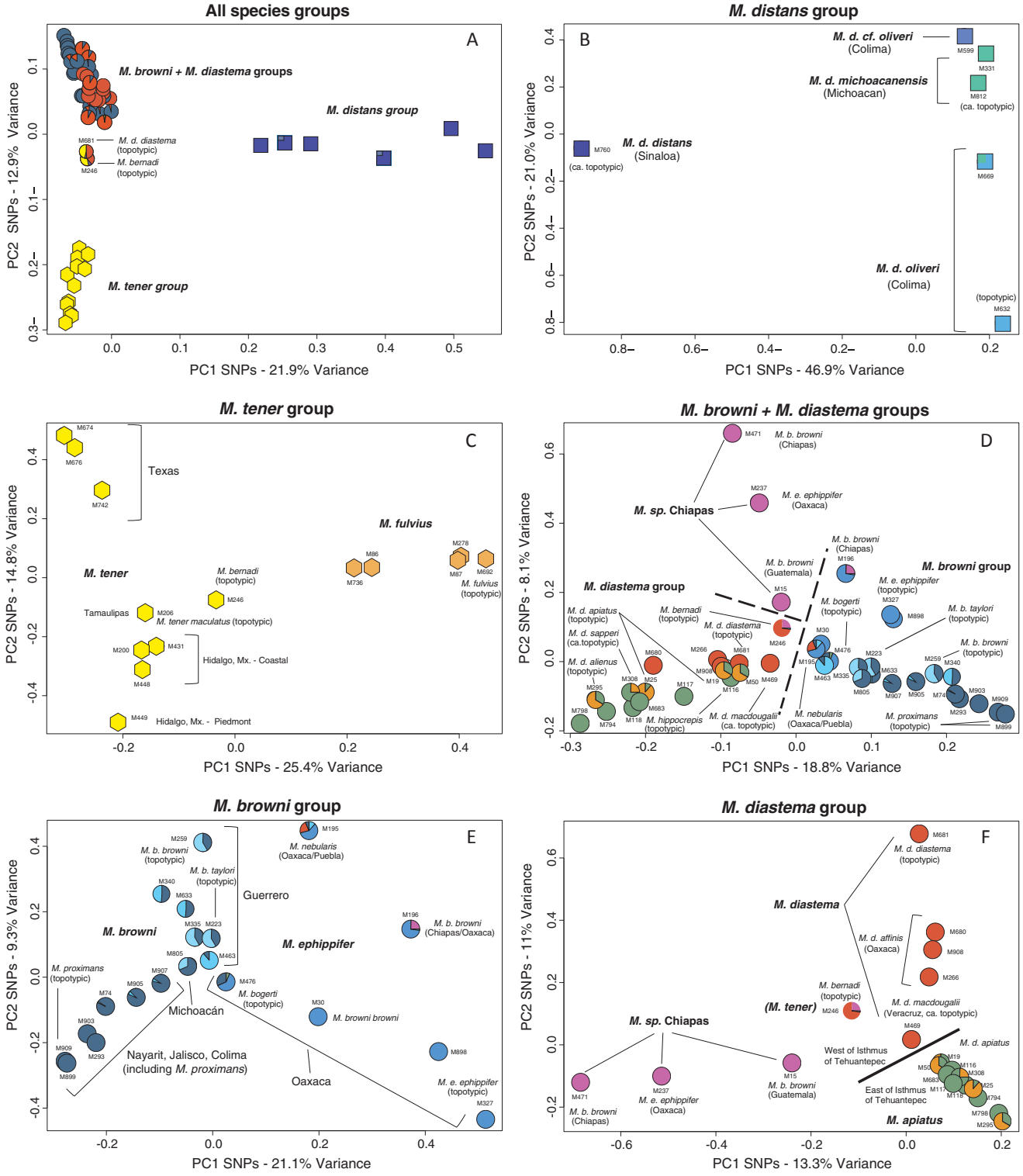

Fig. 5. Principal component analysis (PCA) of 4975 unlinked SNPs obtained from 59 samples included in this study. Plots show PC1 and PC2 for (A) all species and individuals, (B) the *M. distans* group, (C) the *M. tener* group, (D) the *M. browni* and *M. diastema* groups together, (E) the *M. browni* group, and (F) the *M. diastema* group. Individual pie-charts correspond to those of the STRUCTURE analyses depicted in Fig. 4, with all specimens included at $k = 4$, for (A), only *M. distans* group, $k = 4$, for (B), only *M. tener* group, $k = 2$, for (C), and the *M. browni* and *M. diastema* groups at $k = 7$, for (D–F).

Mendes and Hahn, 2017; Roch and Steel, 2014). Our results (i.e., STRUCTURE, SplitsTree and TreeMix) do suggest that gene flow could be pervasive across the *M. diastema* species complex, and may lead to conflicting or misleading phylogenetic resolution of particular groups. Estimated climatic niche models of the distribution of *M. tener* during the Last Glacial Maxima suggest that these species may have inhabited the area presently occupied by *M. proximans* (Streicher et al., 2016), making gene flow between lineages a potential scenario in the recent past. Additionally, sex-biased dispersal is thought to be widespread in Elapids (Keogh et al., 2007), which may underlie sex-biased gene flow that could generate patterns of mito-nuclear conflict. It is notable that the only other study to investigate species boundaries and population

structure using nuclear data for *Micrurus* also identified substantial mito-nuclear conflict within *M. tener* (Streicher et al., 2016). Conclusions from this previous study highlighted the roles of male-biased dispersal and range expansions leading to mitochondrial genetic surfing, and raise the question of whether similar factors may have contributed to the conflicting patterns observed here. Our findings and those of other studies together suggest that the unique biology, dispersal patterns, and evolutionary history of coralsnakes may favor particularly high levels of phylogenetic conflict.

4.3. Bayesian species delimitation

Taken together, our STRUCTURE (Fig. 4) and BFD* (Fig. S5) results suggest multiple instances of both incomplete and complete speciation may exist within the *M. diastema* species complex. Given our current sampling scheme and the assumptions of the method, our species delimitation analyses inferred the largest number of possible species that we tested (i.e., 5 total, 3 sp. for the *M. diastema* group and 2 sp. for *M. browni* group), and yet, our STRUCTURE analyses suggest that many individuals in our RADseq dataset are likely characterized by mixed ancestry. Importantly, the multispecies coalescent model assumes complete absence of gene flow between putative species, which constrains our ability to test the validity of many putative species (e.g., *M. d. alienus*, *M. d. apiatus*) in this group. Our analyses highlight the challenges of determining whether populations should be considered as distinct species or not based solely on limited genetic data alone. Bayesian coalescent-based species delimitation methods, essentially treat population lineages as distinct species in the model, and thus, it seems likely that putative species in the group may be presented as incipient (populations in the early stages of divergence) or the result of isolation by distance by our BFD* analyses, when in fact they are not, as shown by the high levels of admixture suggested by our TreeMix results (Fig. 3C).

4.4. Taxonomic implications

Coloration in snakes is known to be under very strong selection, to the point that multiple snakes of different families converge to the same color pattern (Cox and Davis Rabosky, 2013; Greene and McDiarmid, 1981b; Harper Jr. and Pfennig, 2008; Pfennig et al., 2001a; Rabosky et al., 2016). It is not then surprising that our results are in sharp contrast with the previous taxonomy of this group, which was mostly based on coloration, as differences in predator pressure, Müllerian mimicry, or other factors might result in convergent or divergent color patterns among populations and species. Based on the results of this study we make suggestions regarding the taxonomy of the group. Herein we take a conservative approach at taxonomic change, relying primarily on the preferred structure analysis, $k = 5$, and taking into account samples of mixed ancestry (Fig. 4). We then rely on the Bayesian Species Delimitation (Fig. S5), keeping in mind that most samples with mixed ancestries have been excluded. Third, the phylogenetic analyses, species tree inference using SVDquartets (Fig. 3B) and ML-analysis of SNP data (Fig. 3A), with the last being highly influenced by samples of mixed ancestry. Fourth, the SplitsTree representation (Fig. S2) illustrates mixed ancestry influence and raw distances among samples. Cautiously we also guide our decision with our more extensive (in term of individuals) mtDNA phylogeny, in cases where we lack SNP representation of important taxa (Fig. 2). Combined PCAs of the SNP data represented by the STRUCTURE pie charts for each individual helps us visualize genetic variation (Fig. 5).

4.4.1. The Micrurus distans group

As its name states, this species is distantly related to other members of the *M. diastema* species complex, despite the close resemblance in coloration. Our analysis of mtDNA and nuclear SNPs agree in that our individual from the currently recognized nominotypical subspecies of *M. distans* (Kennicott, 1860) differ substantially from the subspecies to the south, *M. d. michoacanensis* (Duges, 1891) and *M. d. oliveri* Roze, 1967:18. Our mtDNA data set contains two samples of *M. d. zweifeli* Roze, 1967:21, one from southern Nayarit in the Sierra de Pajaritos but just north of the Santiago River, which groups with *M. d. distans*, and the other sample from the mountains of northern Nayarit, grouping with the southern clade. The type locality of *M. d. zweifeli* is located in mountains just south of the Santiago River, a few kilometers south from the Sierra de Pajaritos locality, both localities likely represent the same populations of *M. distans* in these southern mountains. Our sample of *M. d. michoacanensis* gives us contradicting results between the mtDNA and nuclear SNPs, suggesting closer relationships with the nominotypical subspecies in the first and with the southern clade on the second. Unfortunately, our samples of *M. d. michoacanensis* come from the coast of Michoacán, and not from near the type locality in the interior of this state, in the Balsas valley. We assign the specimens to this taxon given the ecologic similarity between the coastal region and the Balsas interior of Michoacan (where the type of *M. d. michoacanensis* is from. Our sample M632 (UTA R-64893) is nearly topotypic from ca. 11 miles (18 km) NW of Periquillo, Colima. Periquillo is the type locality of *M. d. oliveri* (Roze, 1967: 18). Our specimen is a male, just like the type of this taxon, and it coincides almost perfectly in all diagnostic characters including scale counts, with 209 ventral scales (ventrals defined as those scales wider than long; 210 in type) and 52 subcaudal scales (55 in type). The black banding only differs slightly: 9 on body (counting nuchal; 12 in type) and 4 on tail (5 in type). Other diagnostic characters in the original description match perfectly. One specimen, M599, from Colima, does not conform with previous taxa definitions, indicating that further investigation of the Central Colima populations is necessary. Despite the high levels of genetic differentiation between the populations of *M. distans,* the genetic groups that we recovered do not agree completely with current subspecific designations in this species, therefore until further molecular exploration of this group is possible we suggest recognizing at the level of species three of the four subspecies currently used for *M. distans*, one in the north—*M. d. distans* (Kennicott, 1860), including as a synonym typical *M. d. zweifeli* Roze, 1967, one in southern Pacific coast of Jalisco and Colima—*M. d. oliveri* Roze, 1967, and one in the southern Pacific coast of Michoacan and the Balsas Valley—*M. d. michoacanensis* (Duges, 1891) (Fig. 5).

4.4.2. The Micrurus tener group

Streicher et al. (2016) synonymized all subspecies of *M. tener,* as well as *M. tamaulipensis* Lavin-Murcio and Dixon, 2004 and *M. bernadi* (Cope, 1887) with *M. tener* (Baird & Girard, 1853). Our analysis of mtDNA and nuclear SNPs agree with the results of Streicher et al. (2016). Additionally we show that individuals of *M. tener* previously reported from Colima and Morelos (Campbell and Lamar, 2004; Reyes-Velasco et al., 2009) actually represent *M. browni* Schmidt and Smith, 1943. Our phylogenetic analysis of mtDNA recovered multiple individuals from the highlands of Oaxaca (M333, M336, M680) and southern Veracruz (M214) that group with *M. tener*. The individuals from the Pacific versant of Oaxaca (M333 & M336; identified as *M. cf. bogerti*) and Veracruz (M214) were not included in the nuclear SNP analysis, and further work is required to adequately understand their phylogenetic affinities. In our phylogeny of nuclear SNP data, an individual previously identified as *M. bernadi* from Puebla (M246) was sister to *M. tener* + *M. fulvius,* however, a different individual identified as *M. bernadi* (M431) was found nested within *M. tener,* so the taxon *M. bernadi* is confirmed as a synonym of *M. tener*, just as suggested by Streicher et al. (2016), albeit with some admixture with *M. diastema* (Duméril, Bibron, & Duméril, 1854).

4.4.3. The Micrurus diastema group

There is strong evidence to suggest that *M. diastema* is composed of three closely related taxa. Individuals of *M. diastema* that occur west of the isthmus of Tehuantepec represent a single taxon, which includes as

Table 2
Proposed taxonomy support comparison by analytical techniques used in this study. Yes—support for species or species groups according to our structure results and interpretation; No—lack of support for species or species groups; Partial—most but not all samples of a species supported as a unit; NA—support not assessed or when species are predetermined in the analysis according to our proposed taxonomy.

Analysis	*M. apiatus*	*M. browni*	*M. cf. oliveri*	*M. diastema*	*M. distans*	*M. ephippifer*	*M. fulvius*	*M. michoacanensis*	*M. oliveri*	*M. sp.* Chiapas	*M. tener*	*M. browni importunus* not in *M. diastema* complex
Traditional morphological taxonomy (Fig. 2, taxon labels)	No	No	No	No	No	No	Yes	No	No	No	No	No
mtDNA phylogeny (Fig. 2)	Yes	No	No	No	Yes	No	Yes	Yes	No	No	No	Yes
SNP ML phylogeny (Fig. 3A)	Yes	Yes	Yes	Partial	Yes	Partial	Yes	Yes	No	Yes	Yes	Yes
SNP species tree (Fig. 3B)	Yes	NA	NA	NA	NA	NA	NA	NA	NA	NA	NA	NA
SNP TreeMix phylogeny (Fig. 3C)	Yes	NA	NA	NA	NA	NA	NA	NA	NA	NA	NA	NA
SNP splits tree (Fig. S2)	Yes	Yes	Yes	Partial	Yes	Partial	Yes	Yes	No	Yes	Yes	Yes
SNP STRUCTURE k = 4 (*M. distans, M. tener* , and *M. diastema* groups) (Fig. 4)	Yes	Yes	Yes	Yes	Yes	Yes	Yes	Yes	Yes	Yes	Yes	NA
SNP STRUCTURE k = 4 (*M. distans* group) (Fig. 4)	NA	NA	Yes	NA	Yes	NA	NA	Yes	Yes	NA	NA	NA
SNP STRUCTURE k = 2 (*M. tener* group) (Fig. 4)	NA	NA	NA	NA	NA	NA	Yes	NA	NA	NA	Yes	NA
SNP STRUCTURE k = 5 (*M. diastema* group) (Fig. 4)	Yes	Yes	NA	Yes	NA	Yes	NA	NA	NA	Yes	NA	NA
SNP STRUCTURE k = 7 (*M. diastema* group) (Fig. 4)	Yes	Yes	NA	Yes	NA	Yes	NA	NA	NA	Yes	NA	NA
SNP fineRADstructure (Fig. S6)	Yes	Yes	No	Yes	Yes	Yes	Yes	No	No	Yes	Yes	Yes
SNP DAPC (Fig. S3)	Yes	Yes	Yes	Yes	Yes	Yes	Yes	Yes	Yes	Yes	Yes	NA
SNP BFD (*M. browni* and *M. diastema* groups) (Fig. S5)	Yes	Yes	NA	Yes	NA	Yes	NA	NA	NA	Yes	NA	NA
SNP Fst (Table 1)	Yes	Yes	NA	Yes	NA	Yes	Yes	NA	NA	Yes	Yes	NA
SNP PCA (Fig. 5)	Yes	Yes	Yes	Yes	Yes	Yes	Yes	Yes	Yes	Yes	Yes	NA

synonyms the following subspecies currently recognized, *M. d. affinis* (Jan 1858), *M. d. diastema* (Duméril, Bibron & Duméril, 1854) and *M. d. macdougalli* Roze, 1967. The name *M. diastema* (Duméril, Bibron & Duméril, 1854), senior synonym, is applicable to this taxon. The topotypic sample of *M. diastema* is very similar to the type of the species at the MNHN in Paris, and it shows a mixed ancestry of about 30% *M. tener*. Nonetheless, for stability purposes we maintain the name *M. diastema* for this taxon. Individuals previously referred to *M. diastema* that occur east of the isthmus of Tehuantepec form a distinct taxon, which is composed of the currently recognized subspecies, *M. d. alienus* (Werner, 1903:249), *M. d. aglaeope* (Cope, 1860), *M. d. apiatus* (Jan 1858), and *M. d. sapperi* (Werner, 1903:350), and the species *M. hippocrepis* (Peters, 1862) as synonyms. *Elaps apiatus* Jan 1858 has priority, so we suggest the use of the new combination *M. apiatus* (Jan 1858) for populations of these forms. Individuals previously referred to as *M. browni* Schmidt and Smith, 1943 from the Grijalva Valley of the central depression of Chiapas and extreme western Guatemala, and some populations referred to *M. e. ephippifer* (Cope, 1886) due to their dorsal melanic coloration and from the arid eastern Isthmus of Tehuantepec, represent a distinct and undescribed taxon (*M. sp.* Chiapas). The species tree analysis in SVDquartets (Fig. 3B) grouped these individuals with *M. diastema* and *M. apiatus,* just as the mtDNA tree and the SplitsTree analysis (Fig. S2), however the ML analysis of SNP data recovered them as sister to *M. browni*, although with weak support. Additional analyses of morphological characters are necessary in order to revise the taxonomy of these populations.

4.4.4. The Micrurus browni group

We take a conservative taxonomic stance and favor consideration of the *M. browni* group as consisting of two species. We found that most individuals occurring in the west coast of Mexico, from Nayarit to Guerrero, represent a single taxon, *M. browni* Schmidt and Smith, 1943:29. This includes topotypic individuals of the nominotypical subspecies—from Chilpancingo, near topotypic *M. b. taylori* Schmidt and Smith, 1943:30, individuals previously identified as *M. tener fitzingeri* (Jan 1858) from Morelos and Colima, as well as *M. proximans* Smith and Chrapliwy, 1958:270 from Nayarit, Jalisco and Colima. The name *M. browni* Schmidt & Smith, 1943, has priority and is thus applied to this taxon. Individuals identified as *M. b. browni*, *M. e. ephippifer* (Cope, 1886), *M. bogerti* Roze, 1967:9, *M. e. zapotecus* Roze, 1989:11, *M. nebularis* Roze, 1989:9, *M. pachecogili* Campbell, 2000 and some *M. diastema* ssp. from western Oaxaca on the Atlantic versant represent a distinct taxon, for which the senior synonym *M. ephippifer* (Cope, 1886) applies. Two individuals somewhat resembling *M. bogerti* from western Oaxaca showed a *M. tener* mtDNA haplotype (Fig. 2), while the only sample of *M. bogerti* in the nuclear SNP analyses (M476), from the mountains just above the type locality was recovered as sister to *M. browni. Micrurus nebularis* and *M. pachecogili* represent desert highland forms endemic to central Oaxaca and the Zapotitlán basin of Puebla, respectively. Our analyses of nuclear SNP data showed that our *Micrurus nebularis* specimen is sister to all other *M. browni* (Fig. 3A). *Micrurus pachecogili* seems identical to *M. nebularis* on the mtDNA phylogeny, and both placed as part of *M. browni* (Fig. 2), however we were not able to recover useful sequence data from *M. pachecogili* for the ddRADseq analysis but, the almost undistinguishable morphology, habits, and close geographic proximity between the two taxa suggests that they belong to the same population of *M. browni*. Both our samples of *M. nebularis* and *M. bogerti* used in our SNP analyses show mixed ancestry but, close affinity or conspecificity to the taxon *M. ephippifer*. Last, the subspecies *M. b. importunus* Roze, 1967:11 from the highlands of Guatemala is found to be a junior synonym of *M. nigrocinctus zunilensis* Schmidt, 1932.

4.4.5. Methodological reconciliation

We applied a large number of analyses to both mtDNA and ddRADseq data in order to detect species boundaries and to infer relationships among species in the *M. diastema* complex. For the mitochondrial data we generated a Bayesian phylogeny, and we applied a multitude of methods to analyze the nuclear SNP data. These methods are herein discussed and compared in Table 2, according to how they support our preferred species taxonomic arrangement.

The mtDNA Bayesian phylogenetic reconstruction (Fig. 2) exhibits a convoluted signal with little support for either our preferred or traditional morphological taxonomies. Nonetheless, some of the groups are supported (i.e., *M. apiatus, M. distans,* and *M. fulvius*), as well as the placement of *M. browni importunus* within the *M. nigrocinctus* group. For the SNP data, we implemented three phylogenetic analyses, a Maximum Likelihood concatenated approach (RAxML; Fig. 3A), a species tree coalescent method (SVDquartets; Fig. 3B), and a population-based phylogenetic method (TreeMix; Fig. 3C). The ML phylogeny recovers all main taxa recognized, except for those individuals with evidence of mixed ancestry, making the reconstruction and internal support difficult. The other two methods used a reduced number of mixed ancestry individuals, giving a higher support to internal nodes. Nonetheless, the TreeMix phylogeny is able to accommodate estimated patterns of gene flow, both recent and past, among the taxa analyzed, in theory deriving a more robust phylogenetic estimate. Our SplitsTree network (Fig. S2), based on the NeighborNet (neighbor joining) algorithm, depicts the groups obtained by the ML reconstruction, with the exception of individuals with mixed ancestry, which are usually placed between the parental groups.

We also used two model-based cluster analyses (STRUCTURE—Fig. 4, fineRADstructure—Fig. S6) to infer population structure, species assignment, hybrid zones and admixed individuals. The two methods largely coincide and form the backbone of our species delimitation. Additionally, the non-model-based clustering (DAPC—Fig. S3) generally agrees with this depiction of the major groups.

The species delimitation (BFD*—Fig. S5) and the population differentiation quantification (Fst—Table 1) and visualization (PCA—Fig. 5) techniques all supported our preferred species taxonomic

arrangement based on model-based clusters.

In summary, i) all SNP based analyses coincide in defining the major groups among the coralsnakes species studied, and most support at least in part our resulting species designations, ii) we believe each analysis is appropriate and relevant because they provide at least some support or visualization aid for taxonomy, despite their individual limitations but, iii) the model-based clustering techniques (STRUCTURE, fineRADstructure) and phylogenetic analyses incorporating gene flow population data (TreeMix) provide the best guide to understanding population dynamics and species boundaries and inferring phylogenetic relationships on populations under the influence of admixture.

5. Conclusion

At the broadest level, our study illustrates the challenges of species delimitation in this group of morphologically conserved and chromatically diverse snakes. Our data suggest that the current taxonomy of the *M. diastema* species group is not supported by genetic inferences of relatedness and lineage diversity, and requires substantial revision, much of which we address here. Our results also demonstrate that the *M. diastema* species complex is not a monophyletic group, and that fixing the current taxonomic issues in this lineage are not a simple matter of lumping/splitting taxa, but instead a re-assignment and re-organization of taxonomic assignments for individual samples. Our suggestions for a revised taxonomy of this group represent a first major step to rectify the current taxonomy with the evolutionary relationships among populations and lineages within this group. However, a number of populations and lineages remain largely unsampled, or were sparsely sampled in this study, which warrant future investigations to determine species boundaries.

CRediT authorship contribution statement

Jacobo Reyes-Velasco: Laboratory work, Formal analysis, Resources, Software, Validation. **Richard H. Adams:** Formal analysis, Software, Validation. **Stephane Boissinot:** Resources, Supervision. **Christopher L. Parkinson:** Funding acquisition, Resources. **Jonathan A. Campbell:** Funding acquisition, Resources. **Todd A. Castoe:** Conceptualization, Funding acquisition, Resources, Supervision, Visualization. **Eric N. Smith:** Conceptualization, Funding acquisition, Resources, Supervision, Visualization.

Declaration of Competing Interest

The authors declare that they have no known competing financial interests or personal relationships that could have appeared to influence the work reported in this paper.

Acknowledgments

We thank members of the Campbell, Castoe and Smith labs at UTA for their helpful suggestions. We thank multiple Institutions and individuals for providing tissues for this study or for their help in the field, including Rafael Aguilar Cortes, Alejandro Carbajal Saucedo, Ivan Ahumada-Carrillo, Oscar Avila, Luis Canseco, Eric Centenero Alcalá, Christian Cox, Tom Devitt, the late James R. Dixon, Oscar Flores-Villela, Carl Franklin, Uri García, Chistoph Grünwald, Cristián Guirola, Alexander Hermosillo, Carlos Hernandez, Raul Hernandez Arciga, Salomon Hernandez G, Jason Jones, Kenneth Krysko, David Lazcano Villareal, Jesus Loc-Barragan, Victor Luja, Cesar Márquez Camargo, Elizabeth A. Martínez-Salazar, Oscar Medina, Jessee M. Meik, Andrés Alberto Mendoza-Hernández, the late Fernando Mendoza-Quijano, F. Ricardo Mendoza Paz, Roberto Mora, Robert Murphy, Adrian Nieto-Montes de Oca, Ivel Orozco, Carlos Pavón, Gil Paz Gutiérrez, Ricardo Pérez, Edmundo Perez-Ramos, Paulino Ponce-Campos, Quetzal Pureco Rivera, Antonio Ramírez-Velázquez, Jorge Quezada Hipolito, Andrea Roth Monzón, Aide Rodriguez Tiburcio, Mahmood Sasa, Coleman Sheehy, Carlos Soto, Ireri Suazo Ortuño, Jonatan Torres Pérez, Manuel Varela, Jens Vindum, Coleman Sheehy, Ginny Weatherman and Gabriela Zamora-Silva. Isaac Overcast provided valuable assistance with ipyrad, and Joseph Manthey and Yann Bourgeois provided assistance with data analyses. Collecting permits were issued by the Dirección de la Fauna Silvestre to JAC and the Secretaria de Medio Ambiente y Recursos Naturales (SEMARNAT) to J. L. Camarillo-Rangel, V. León-Règagnon, and Oscar Flores-Villela. Funding for this project was provided by NSF grants to CLP and ENS (DEB-0416000 & 0416160), and JAC (DEB-0613802 & 0102383), a grant from Instituto Bioclon to ENS, faculty startup funds from the University of Texas at Arlington to TAC, a Theodore Roosevelt Memorial Fund Grant from the American Museum of Natural History to JRV, and by faculty startup funds from NYUAD to SB.

Appendix A. Supplementary material

Supplementary data to this article can be found online at https://doi.org/10.1016/j.ympev.2020.106770.

References

Adams, R.H., Schield, D.R., Card, D.C., Castoe, T.A., 2018. Assessing the impacts of positive selection on coalescent-based species tree estimation and species delimitation. Syst. Biol. 67, 1076–1090.
Arèvalo, E., Davis, S.K., Sites Jr, J.W., 1994. Mitochondrial DNA sequence divergence and phylogenetic relationships among eight chromosome races of the Sceloporus grammicus complex (Phrynosomatidae) in central Mexico. Syst. Biol. 43, 387–418.
Bouckaert, R., Heled, J., Kühnert, D., Vaughan, T., Wu, C.-H., Xie, D., Suchard, M.A., Rambaut, A., Drummond, A.J., 2014. BEAST 2: a software platform for Bayesian evolutionary analysis. PLoS Comput. Biol. 10, e1003537.
Brodie III, E., Janzen, F., 1995. Experimental studies of coral snake mimicry: generalized avoidance of ringed snake patterns by free-ranging avian predators. Funct. Ecol. 186–190.
Brodie III, E.D., 1993. Differential avoidance of coral snake banded patterns by free-ranging avian predators in Costa Rica. Evolution 227–235.
Campbell, J.A., Lamar, W.W., 2004. The Venomous Reptiles of the Western Hemisphere. Comstock Pub Associates Ithaca.
Castoe, T.A., de Koning, A.J., Kim, H.-M., Gu, W., Noonan, B.P., Naylor, G., Jiang, Z.J., Parkinson, C.L., Pollock, D.D., 2009. Evidence for an ancient adaptive episode of convergent molecular evolution. Proc. Natl. Acad. Sci. 106, 8986–8991.
Castoe, T.A., Smith, E.N., Brown, R.M., Parkinson, C.L., 2007. Higher-level phylogeny of Asian and American coralsnakes, their placement within the Elapidae (Squamata), and the systematic affinities of the enigmatic Asian coralsnake Hemibungarus calligaster (Wiegmann, 1834). Zool. J. Linn. Soc. 151, 809–831.
Castoe, T.A., Streicher, J.W., Meik, J.M., Ingrasci, M.J., Poole, A.W., de Koning, A.P., Campbell, J.A., Parkinson, C.L., Smith, E.N., Pollock, D.D., 2012. Thousands of microsatellite loci from the venomous coralsnake Micrurus fulvius and variability of select loci across populations and related species. Mol. Ecol. Resour. 12, 1105–1113.
Chifman, J., Kubatko, L., 2014. Quartet inference from SNP data under the coalescent model. Bioinformatics 30, 3317–3324.
Cox, C.L., Davis Rabosky, A.R., 2013. Spatial and temporal drivers of phenotypic diversity in polymorphic snakes. Am. Nat. 182, E40–E57.
Danecek, P., Auton, A., Abecasis, G., Albers, C.A., Banks, E., DePristo, M.A., Handsaker, R.E., Lunter, G., Marth, G.T., Sherry, S.T., 2011. The variant call format and VCFtools. Bioinformatics 27, 2156–2158.
Drummond, A.J., Rambaut, A., 2007. BEAST: Bayesian evolutionary analysis by sampling trees. BMC Evolut. Biol. 7.
Eaton, D.A., Overcast, I., 2017. ipyrad: interactive assembly and analysis of RADseq.
Edgar, R.C., 2004. MUSCLE: multiple sequence alignment with high accuracy and high throughput. Nucl. Acids Res. 32, 1792–1797.
Evanno, G., Regnaut, S., Goudet, J., 2005. Detecting the number of clusters of individuals using the software STRUCTURE: a simulation study. Mol. Ecol. 14, 2611–2620.
Fraser, D.F., 1973. Variation in the coral snake *Micrurus diastema*. Copeia 1–17.
Good, J.M., Hird, S., Reid, N., Demboski, J.R., Steppan, S.J., Martin-Nims, T.R., Sullivan, J., 2008. Ancient hybridization and mitochondrial capture between two species of chipmunks. Mol. Ecol. 17, 1313–1327.
Gordon, A., Hannon, G., 2010. Fastx-toolkit. FASTQ/A short-reads preprocessing tools (unpublished) http://hannonlab.cshl.edu/fastx_toolkit.
Greene, H.W., McDiarmid, R.W., 1981a. Coral snake mimicry: does it occur. Science 213, 1207–1212.
Greene, H.W., McDiarmid, R.W., 1981b. Coral snake mimicry: does it occur? Science 213, 1207–1212.
Guo, P., Liu, Q., Xu, Y., Jiang, K., Hou, M., Ding, L., Pyron, R.A., Burbrink, F.T., 2012. Out of Asia: Natricine snakes support the Cenozoic Beringian Dispersal Hypothesis. Mol. Phylogenet. Evol. 63, 825–833.
Harper Jr, G.R., Pfennig, D.W., 2008. Selection overrides gene flow to break down maladaptive mimicry. Nature 451, 1103.

Holman, J.A., 2000. Fossil Snakes of North America: Origin, Evolution, Distribution, Paleoecology. Indiana University Press.
Huelsenbeck, J.P., Ronquist, F., 2001. MRBAYES: Bayesian inference of phylogenetic trees. Bioinformatics 17, 754–755.
Huson, D.H., Bryant, D., 2005. Estimating phylogenetic trees and networks using SplitsTree 4. Manuscript in preparation, software available from www.splitstree.org.
Huson, D.H., Bryant, D., 2006. Application of phylogenetic networks in evolutionary studies. Mol. Biol. Evol. 23, 254–267.
Jombart, T., 2008. adegenet: a R package for the multivariate analysis of genetic markers. Bioinformatics 24, 1403–1405.
Jombart, T., Devillard, S., Balloux, F., 2010. Discriminant analysis of principal components: a new method for the analysis of genetically structured populations. BMC Genet. 11, 94.
Jowers, M.L., Garcia Mudarra, J.L., Charles, S.P., Murphy, J.C., 2019. Phylogeography of West Indies coral snakes (*Micrurus*): Island colonization and banding patterns. Zool. Scr. 48, 263–276.
Kelly, C.M.R., Barker, N.P., Villet, M.H., Broadley, D.G., 2009. Phylogeny, biogeography and classification of the snake superfamily Elapoidea: a rapid radiation in the late Eocene. Cladistics 25, 38–63.
Keogh, J.S., 1998. Molecular phylogeny of elapid snakes and a consideration of their biogeographic history. Biol. J. Linn. Soc. 63, 177–203.
Keogh, J.S., Webb, J.K., Shine, R., Keogh, J.S., J. K. Webb, and R. Shine., 2007. Spatial genetic analysis and long-term mark-recapture data demonstrate male-biased dispersal in a snake. Biol. Lett. 3, 33–35.
Kubatko, L.S., Degnan, J.H., 2007. Inconsistency of phylogenetic estimates from concatenated data under coalescence. Syst. Biol. 56, 17–24.
Lanfear, R., Calcott, B., Ho, S.Y., Guindon, S., 2012. Partitionfinder: combined selection of partitioning schemes and substitution models for phylogenetic analyses. Mol. Biol. Evol. 29, 1695–1701.
Lavin-Murcio, P.A., Dixon, J.R., 2004. A new species of coral snake (Serpentes, Elapidae) from the Sierra de Tamaulipas, Mexico. Phyllomedusa: J. Herpetol. 3, 3–7.
Leaché, A.D., Chavez, A.S., Jones, L.N., Grummer, J.A., Gottscho, A.D., Linkem, C.W., 2015. Phylogenomics of phrynosomatid lizards: conflicting signals from sequence capture versus restriction site associated DNA sequencing. Genome Biol. Evolut. 7, 706–719.
Leaché, A.D., Fujita, M.K., Minin, V.N., Bouckaert, R.R., 2014. Species delimitation using genome-wide SNP data. Syst. Biol. 63, 534–542.
Malinsky, M., Trucchi, E., Lawson, D.J., Falush, D., 2018. RADpainter and fineRADstructure: population inference from RADseq data. Mol. Biol. Evol. 35, 1284–1290.
Meirmans, P.G., 2015. Seven common mistakes in population genetics and how to avoid them. Mol. Ecol. 24, 3223–3231.
Mendes, F.K., Hahn, M.W., 2016. Gene tree discordance causes apparent substitution rate variation. Syst. Biol. 65, 711–721.
Mendes, F.K., Hahn, M.W., 2017. Why concatenation fails near the anomaly zone. Syst. Biol. 67, 158–169.
Miller, M.A., Pfeiffer, W., Schwartz, T., 2010. Creating the CIPRES Science Gateway for inference of large phylogenetic trees. Gateway Computing Environments Workshop (GCE), 2010. IEEE, pp. 1–8.
Novembre, J., Johnson, T., Bryc, K., Kutalik, Z., Boyko, A.R., Auton, A., Indap, A., King, K.S., Bergmann, S., Nelson, M.R., Stephens, M., Bustamante, C.D., 2008. Genes mirror geography within Europe. Nature 456, 98–103.
Parkinson, C.L., Campbell, J.A., Chippindale, P.T., 2002. Multigene phylogenetic analyses of pitvipers, with comments on their biogeography. In: Schuett, G.W., Höggren, M., Douglas, M.E., Greene, H.W. (Eds.), Biology of the vipers. Eagle Mountain Publishing, Eagle Mountain, Utah, pp. 93–110.
Peterson, B.K., Weber, J.N., Kay, E.H., Fisher, H.S., Hoekstra, H.E., 2012. Double digest RADseq: an inexpensive method for de novo SNP discovery and genotyping in model and non-model species. PLoS ONE 7, e37135.
Pfennig, D.W., Harcombe, W.R., Pfennig, K.S., 2001a. Frequency-dependent Batesian mimicry. Nature 410, 323.
Pfennig, D.W., Harcombe, W.R., Pfennig, K.S., 2001b. Frequency-dependent batesian mimicry - predators avoid look-alikes of venomous snakes only when the real thing is around. Nature 410, 323.
Pickrell, J.K., Pritchard, J.K., 2012. Inference of population splits and mixtures from genome-wide allele frequency data. PLoS Genet. 8, e1002967.
Pritchard, J.K., Stephens, M., Donnelly, P., 2000. Inference of population structure using multilocus genotype data. Genetics 155, 945–959.
Rabosky, A.R.D., Cox, C.L., Rabosky, D.L., Title, P.O., Holmes, I.A., Feldman, A., McGuire, J.A., 2016. Coral snakes predict the evolution of mimicry across New World snakes. Nature Commun. 7.
Rambaut, A., Suchard, M.A., Xie, D., Drummond, A.J., 2014. Tracer v1.6. http://beast.bio.ed.ac.uk/Tracer.
Rannala, B., Yang, Z., 2008. Phylogenetic inference using whole genomes. Annu. Rev. Genomics Hum. Genet. 9, 217–231.
Renjifo, C., Smith, E.N., Hodgson, W.C., Renjifo, J.M., Sanchez, A., Acosta, R., Maldonado, J.H., Riveros, A., 2012. Neuromuscular activity of the venoms of the Colombian coral snakes *Micrurus dissoleucus* and *Micrurus mipartitus*: An evolutionary perspective. Toxicon 59, 132–142.
Reyes-Velasco, J., Hermosillo-López, I., Grunwald, C., Ávila-López, O., 2009. New state records for amphibians and reptiles from Colima, Mexico. Herpetol. Rev. 40, 117.
Roch, S., Steel, M., 2014. Likelihood-based tree reconstruction on a concatenation of alignments can be positively misleading. arXiv preprint arXiv:1409.2051.
Roze, J., 1967. A checklist of the new world venomous coral snakes (Elapidae), with descriptions of new forms. Am. Mus. Novit. 1–60.
Roze, J.A., 1996. Coral Snakes of the Americas. Krieger Publishing Company, Malabar, Florida.
Slowinski, J.B., 1995. A phylogenetic analysis of the New World coral snakes (Elapidae: Leptomicrurus, Micruroides, and Micrurus) based on allozymic and morphological characters. J. Herpetol. 325–338.
Slowinski, J.B., Keogh, J.S., 2000a. Phylogenetic relationships of elapid snakes based on cytochrome mtDNA sequences. Mol. Phylogenet. Evol. 15, 157–164.
Slowinski, J.B., Keogh, J.S., 2000b. Phylogenetic relationships of elapid snakes based on cytochrome *b* mtDNA sequences. Mol. Phylogenet. Evol. 15, 157–164.
Smith, S.M., 1975. Innate recognition of coral snake pattern by a possible avian predator. Science 187, 759–760.
Smith, S.M., 1977. Coral-snake pattern recognition and stimulus generalisation by naive great kiskadees (Aves: Tyrannidae). Nature 265, 535.
Som, A., 2014. Causes, consequences and solutions of phylogenetic incongruence. Briefings Bioinf. 16, 536–548.
Stamatakis, A., 2014. RAxML version 8: a tool for phylogenetic analysis and post-analysis of large phylogenies. Bioinformatics 30, 1312–1313.
Streicher, J.W., McEntee, J.P., Drzich, L.C., Card, D.C., Schield, D.R., Smart, U., Parkinson, C.L., Jezkova, T., Smith, E.N., Castoe, T.A., 2016. Genetic surfing, not allopatric divergence, explains spatial sorting of mitochondrial haplotypes in venomous coralsnakes. Evolution 70, 1435–1449.
Streicher, J.W., Schulte, J.A., Wiens, J.J., 2015. How should genes and taxa be sampled for phylogenomic analyses with missing data? An empirical study in iguanian lizards. Syst. Biol. 65, 128–145.
Swofford, D.L., 2003. {PAUP*. Phylogenetic analysis using parsimony (* and other methods). Version 4.}.
Team RStudio, R., 2015. RStudio: integrated development for R. RStudio, Inc., Boston, MA URL http://www.rstudio.com 42, 14.
Uetz, P., Jirí, H., 2015. The Reptile Database.
Vaidya, G., Lohman, D.J., Meier, R., 2011. SequenceMatrix: concatenation software for the fast assembly of multi-gene datasets with character set and codon information. Cladistics 27, 171–180.
Valencia, J.H., Garzón-Tello, K., Barragán-Paladines, M.E., 2016. Serpientes Venenosas del Ecuador: Sistemática, Taxonomía, Historia Natural, Conservación, Envenenamiento y Aspectos Antropológicos. Fundación Herpetológica Gustavo Orcés, Universidad de Texas-Arlington, Fondo Ambiental Nacional, Quito.
Yang, Z., Rannala, B., 2010. Bayesian species delimitation using multilocus sequence data. Proc. Natl. Acad. Sci. 107, 9264–9269.
Zhang, C., Zhang, D.-X., Zhu, T., Yang, Z., 2011. Evaluation of a Bayesian coalescent method of species delimitation. Syst. Biol. 60, 747–761.
Zweifel, R.G., 1959. Additions to the herpetofauna of Nayarit, Mexico. American Museum Novitates 1–13.